Swimming bacteria power microscopic gears

Andrey Sokolov[a,b], Mario M. Apodaca[c], Bartosz A. Grzybowski[c,d,1], and Igor S. Aranson[a,e,1]

[a]Materials Science Division, Argonne National Laboratory, Argonne, IL 60439; [b]Department of Ecology and Evolutionary Biology, Princeton University, Princeton, NJ 08543; and [c]Departments of Chemistry, [d]Chemical and Biological Engineering, and [e]Engineering Sciences and Applied Mathematics, Northwestern University, 2145 Sheridan Rd, Evanston, IL 60208

Communicated by George W. Crabtree, Argonne National Laboratory, Argonne, IL, November 11, 2009 (received for review October 20, 2009)

Whereas the laws of thermodynamics prohibit extraction of useful work from the Brownian motion of particles in equilibrium, these motions can be "rectified" under nonequilibrium conditions, for example, in the presence of asymmetric geometrical obstacles. Here, we describe a class of systems in which aerobic bacteria *Bacillus subtilis* moving randomly in a fluid film power submillimeter gears and primitive systems of gears decorated with asymmetric teeth. The directional rotation is observed only in the regime of collective bacterial swimming and the gears' angular velocities depend on and can be controlled by the amount of oxygen available to the bacteria. The ability to harness and control the power of collective motions appears an important requirement for further development of mechanical systems driven by microorganisms.

collective behavior | ratchet | self-propulsion | sustained rotation

The laws of thermodynamics prohibit extraction of useful work from the Brownian motion of molecules or particles in systems at equilibrium (nonexistence of a perpetuum mobile of the second kind or Maxwell demon) (1, 2). When, however, such randomly moving objects interact with certain types of time-varying external potentials (3–5) or with asymmetric geometrical obstacles under nonequilibrium conditions (6–10), their motions can be "rectified" and made directional. This phenomenon, first considered by Smoluchowski (11) and then analyzed in detail by Feynman (1), underlies the operation of so-called Brownian ratchets and motors (12–15). The examples of biological "Brownian motors" include kinesin and myosin proteins converting chemical energy into directed motion on microtubules (16), and bacteria propelling themselves in viscous fluid owing to the "asymmetry"/chirality of flagellar rotation (14, 17). In man-made systems, ratcheting in asymmetric, funnel-like microchannels has been used to guide bacteria (18) and to sort cancerous from noncancerous cells (18, 19). Recently, there has been interest in using randomly moving bacteria (20), cells (21), or even extracts of cellular cytoskeleton (22, 23) to serve as "biological fuel" powering mechanical micromachines—for instance, systems of microscopic gears. Although recent theoretical work (24) indicates that the vision of such machines is within the realm of possibility, there have been no experimental demonstrations, save the arrangements in which the motions of the bacteria/cells have been preorganized using microfluidic channels (9, 20, 25–28).

In this paper we describe a class of systems in which common aerobic motile bacteria *Bacillus subtilis* moving randomly in a thin fluid film power submillimeter gears and primitive systems of gears decorated with asymmetric teeth (Fig. 1*A* and *B*). Whereas the gear's center of mass exhibits apparent random motion, the gears are spun in the direction determined by the gear's asymmetry, i.e. orientation of the teeth's slanted edges. Remarkably, directional rotation of the gears is observed only in the regime of collective bacterial swimming and the gears' angular velocities depend on and can be controlled by the amount of oxygen available to the bacteria.

Many motile bacteria are known to execute random motions due to "run-and-tumble" processes reminiscent of the Brownian motion of molecules in fluids (29). In the context of thermodynamics, suspensions of such bacteria are often viewed as a "bacterial bath" (30) for which, however, the probability distribution of velocities and the nature of fluctuations are markedly different than those of the "thermal bath" in equilibrium systems. The nonequilibrium character of swimming bacteria is even more manifest at high volume fractions, where diffusion of tracers and oxygen is greatly enhanced (30, 31), up to sevenfold reduction of viscosity is observed (32), and the onset of large-scale collective motions caused by purely hydrodynamic interactions between the bacteria is seen (33–35). Nonequilibrium properties of the bacterial bath are evidenced, for example, by the distribution function $P(V)$ for the velocities of small fluorescent tracer particles V advected by the bacteria in the regime of collective swimming. Fig. 1*C* illustrates that such a distribution for bacteria *Bacillus subtilis* is markedly non-Gaussian (anticipated for fluids at equilibrium), has kurtosis about 0.47, and is approximated by a stretched exponential. We hypothesized that these characteristics—especially the transition to collective swimming—can enable creation of machines in which bacteria move objects millions of times more massive than themselves (here, mass of a gear used $\sim 6 \times 10^{-6}$ g vs. mass of a bacterium 2×10^{-12} g). Recent theoretical work by Angelani et al. (24) on bacteria interacting with asymmetric gears gives credence to our assumption, although it does not provide any hints as to the putative importance of collective swimming.

Results

Our experimental system comprised gears approximately 380 μm in diameter and 50 μm thick and presenting asymmetric teeth; gears with symmetric teeth were also fabricated for control experiments. The gears were made of SU-8 photoresist (MicroChem Corporation) by conventional photolithography (see *Materials and Methods*) and differed in the number, shape, and arrangement (outer vs. inner) of the teeth—some designs we tested are shown in Fig. 1*A*. Approximately 400 gears of each type were prepared on a single silicon wafer.

The gears were placed in suspensions of aerobic swimming bacteria *Bacillus subtilis* confined to thin, freestanding liquid films (Fig. 1*B* and *Materials and Methods*). Because the gears were approximately two times denser than the bacterial broth, they sank to the lower fluid/air interface. Also, because the films were slightly concave, the gears migrated, due to gravity, toward the center of the film. In most experiments, the film thickness was approximately 200–300 μm, and the concentration of bacteria was on the order of 2×10^{10} cm^{-3}—that is, about 20 times higher than in the stationary phase of growth for *Bacillus subtilis*. Experiments were also performed for different concentrations. To control the swimming speed of aerobic bacteria, the chamber housing the film was filled either with oxygen (promoting swimming) or with nitrogen (inhibiting swimming).

Author contributions: B.A.G. and I.S.A. designed research; A.S. and M.M.A. performed research; M.M.A. contributed new reagents and analytic tools; A.S. and I.S.A. analyzed data; and A.S., M.M.A., B.A.G., and I.S.A. wrote the paper.

The authors declare no conflict of interest.

[1]To whom correspondence may be addressed. E-mail: aranson@anl.gov or grzybor@northwestern.edu.

This article contains supporting information online at www.pnas.org/cgi/content/full/0913015107/DCSupplemental.

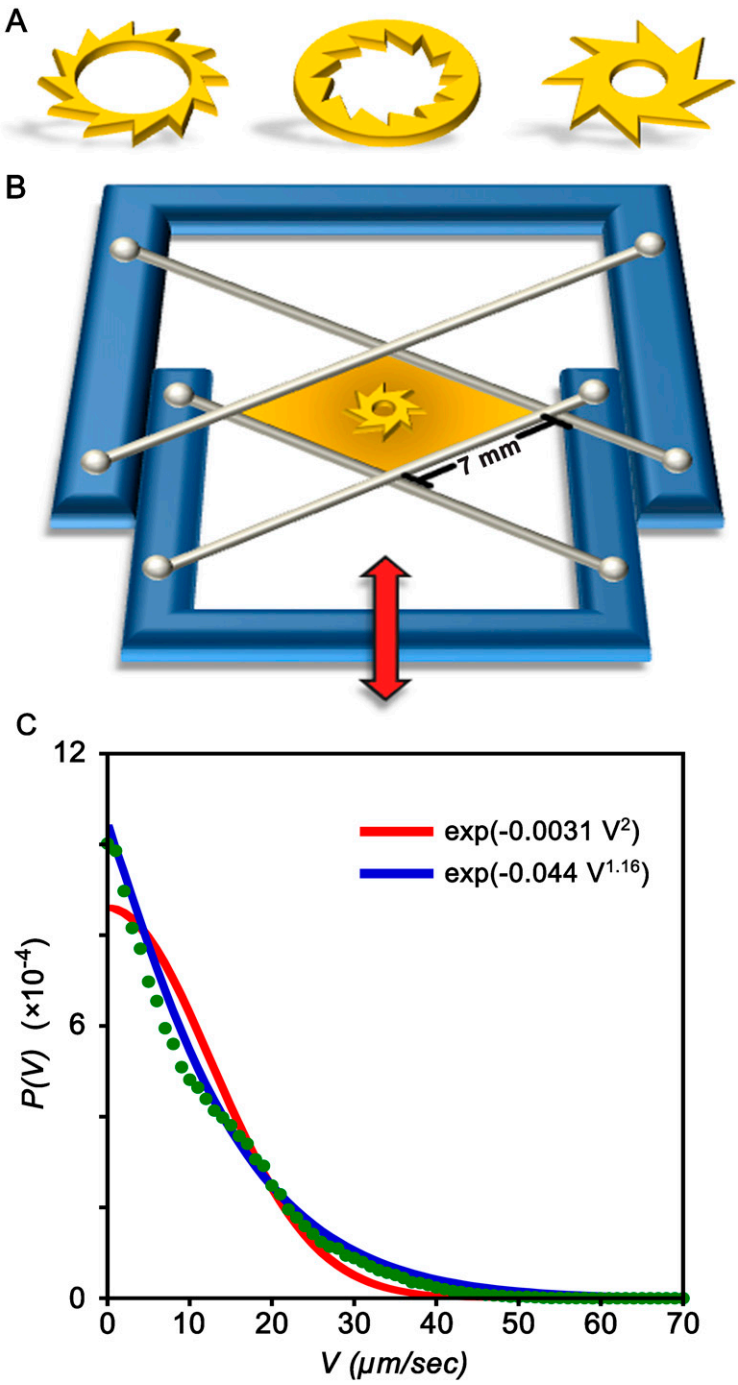

Fig. 1. Experimental design. (*A*) Shapes of some types of gears used in this study. (*B*) Scheme of the experimental setup. The film is suspended between four wires attached to a moveable frame. Film thickness is controlled by the linear motion of the frame (indicated by the red arrow). The experimental apparatus is placed in a transparent chamber with controlled atmosphere and mounted on the moving stage of inverted microscope. (*C*) Velocity distribution function $P(V)$ for small fluorescent tracers (2.5 μm polystyrene microspheres, Spherotech, Inc.) advected by *Bacillus subtilis* bacteria in the regime of collective swimming at concentration 2×10^{10} cm^{-3}. Corresponding rms velocity, V_{rms}, of the tracers is about 13 μm/sec. Red line gives the best fit to the Gaussian law, and blue line is a stretched exponential fit with the exponent 1.16.

No rotation was observed either for gears having symmetric teeth or for relatively low concentrations ($\sim 10^9$ cm^{-3}) of bacteria. The gears rotated only if (*i*) their teeth, either outer or inner, were asymmetric (i.e., one of their edges was more slanted than the other with respect to the radial coordinate); and (*ii*) the concentration of bacteria was in the range of $1–4 \times 10^{10}$ cm^{-3}, which corresponds to the regime of collective swimming (31–34) and is characterized by a formation of self-organized, large-scale vortices of bacterial locomotion and intermittent three-dimensional plume-like structures of increased concentration of bacteria in the bulk of the film (manifested as dark spots on the surface of the film). The characteristic size of these vortices and plume-like structures is approximately 50–100 μm, i.e. still several times smaller than the gear's diameter. In Movies S1 and S2, the plumes manifest themselves as dark moving spots on the film's surface (31).

The rotation of gears was always in the direction of the teeth's slanted edges and the average angular velocities were

approximately 1–2 rpm (see Fig. 2). The rotation rates depended on the concentration of bacteria, the gear's size, and the number and form of the gear's teeth. On the other hand, variations of film thickness had no noticeable effect on the rotation rates as long as the film was thicker than 200 μm, i.e. 3–4 times of the gear's thickness. Both the rotational velocity and the position of the gear's center of mass showed significant fluctuations. However, fluctuations of the rotation rate decreased with the increase in the number of teeth—for example, the gear with 12 teeth rotated more "smoothly" than that with 8 teeth (Fig. 3*A* and *B* and Movies S1 and S2). Also, we verified that gear rotation was not due to any external disturbances but rather due to bacterial motions. This was confirmed by experiments in which the chamber was filled with nitrogen—under these anaerobic conditions, the gears stopped rotating (Fig. 3*C*). When, however, the chamber was refilled with oxygen, the gears started rotating again.

The bacteria could move more than one gear. Fig. 2*I* and *J* and Movie S3 show a system in which two gears of opposite "chiralities" of the teeth were placed into the film and, by gravity, migrated toward the film's center. Once close to one another, the gears interdigitated their teeth and started rotating in synchrony for almost 100 sec (Fig. 3*D*) but in opposite directions. As in the case of individual gears, the rotation of the two-gear system could be controlled by the flow of nitrogen/oxygen through the bacterial broth.

In both one- and two-gear systems, the gears gradually slowed down and after 6–8 min finally came to a complete halt. This deceleration can be attributed to the combination of several effects: (*i*) consumption of nutrients necessary to sustain bacterial swimming, (*ii*) slow evaporation of the fluid film, and (*iii*) secretion of bacterial surfactants that increase the viscosity of the liquid (36) and contribute to the formation of semisolid layers [observed in earlier studies (31, 35)] at the top and bottom liquid/air interfaces. These layers introduce dry friction and a certain threshold for the amplitude of force necessary to turn the gear.

We also studied the dependence of gear rotation rate on the concentration of bacteria; the results of these studies are summarized in Fig. 4. Here, we observed sharp increase in the rotation rate above concentration around 10^{10} cm^{-3}. Importantly, this concentration level is very close to the onset of collective motion established by earlier studies (31, 32). Moreover, for concentration levels above $4–5 \times 10^{10}$ cm^{-3} the gears stop rotating. As reported in our previous work (32), these levels correspond to a slowdown and then complete cessation of the bacterial motility. These effects are likely related to the onset of quorum sensing and biofilm formation. The increase in the rotation rate with increasing concentration coincides with a marked decrease in the effective viscosity of the suspension that is also related to the onset of collective motion (32), as shown by the red line in Fig. 4. Compared with the viscosity of the pure medium, ν_0, the viscosity in the regime of well-developed collective swimming (i.e., bacterial concentration $1–4 \times 10^{10}$ cm^{-3}) drops by a factor of seven even before increasing for highly concentrated bacterial suspensions. These results emphasize the importance of the bacterial collective motions in affecting gear rotation.

Discussion

Collective swimming may greatly increase the momentum transfer from the bacterial bath to the gear. In principle, this hypothesis could be verified by tracking the trajectories of individual bacteria—under high-concentration conditions, however, such tracking proved technically impossible. Instead, we followed the trajectories of small (2.5 μm) fluorescent tracers added to bacterial suspension, Fig. 5. The tracer particles often attach permanently to bacteria, making them perfect markers of bacterial motion. As illustrated in Fig. 5*A*, far away from the gear, the tracers trajectories mainly "decorate" large-scale fluid velocity field.

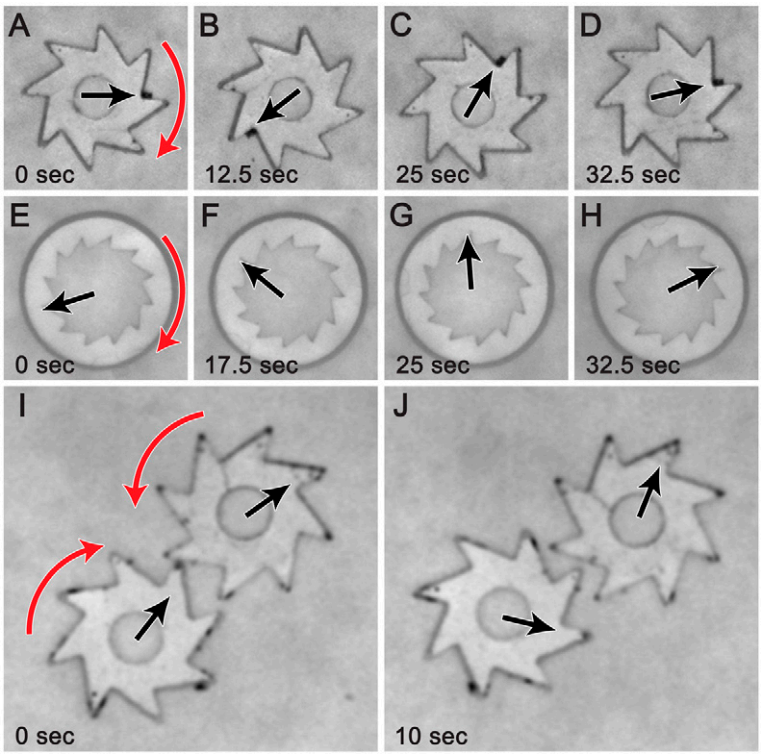

Fig. 2. Rotation of individual gears and of gear assemblies. Sequences of snapshots illustrating rotation of gears with eight external teeth (*A–D*) and twelve internal teeth (*E–H*). Images (*I*) and (*J*) show a system of two "engaged" gears rotating in opposite directions. Black arrows indicate the gears' orientation obtained by computer processing of acquired images, and red arrows show the direction of rotation. In all cases, concentration of bacteria was 2×10^{10} cm^{-3} and the film thickness was 200 μm. Contrast of the images was adjusted electronically. Movies S1, S2, and S3 correspond to images *A–J*.

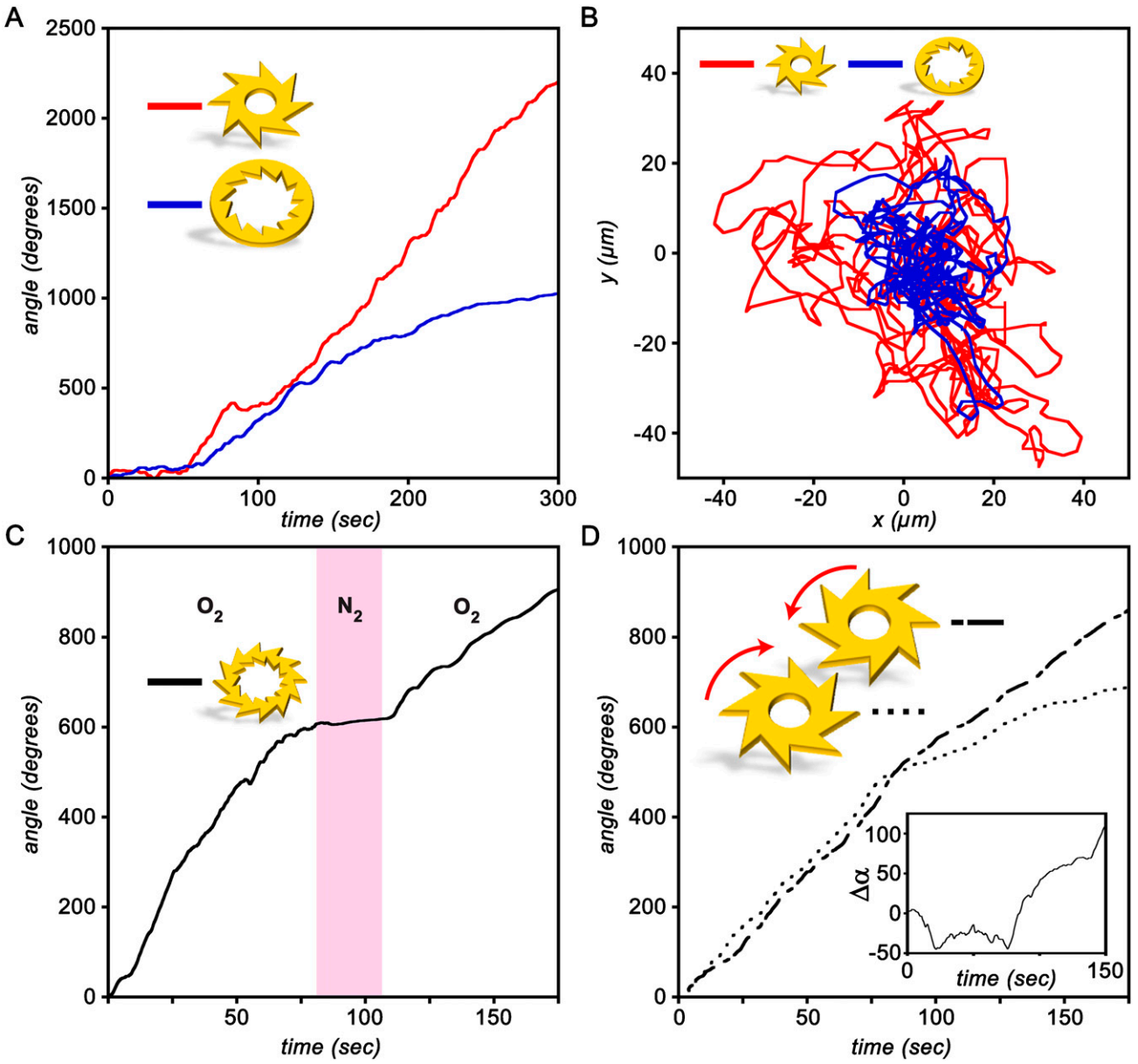

Fig. 3. Quantification of gear performance. (*A*) Gear's rotation. Typical plots of the rotation angle vs. time for two types of gears. (*B*) Random motion of the center of mass. Position of the gears' center of mass for the data shown in (*A*). Gears fluctuate around the center of the film due to confinement caused by the gravitational depression of the film. (*C*) Speed control. Plot of the rotation angle as a function of time for a gear with both internal and external teeth. The gear rotates when bacteria are exposed to air or oxygen but halt (region shaded pink) when the chamber is filled with nitrogen. (*D*) Synchronous rotation. Rotation angle as a function of time for a system of two gears. For approximately the first 100 sec, the gears rotate in synchrony. The inset plots the difference $\Delta\alpha$ in the rotation angles. Movies S1 and S2 accompany data in (*A*) and (*B*), Movie S4 accompanies data in (*C*), and Movie S3 accompanies data in (*D*).

In the proximity of the gear, however, tracers slide along the slanted edges of the gear's teeth and become trapped in the corners at the teeth's junctions (Fig. 5*B–F*) for extended periods of time before finally escaping these "traps." Because bacteria attached to the tracers are self-propelled objects, they push the tracers against the gear wall during the trapping events and effectively transfer momentum to the gear, see also Movie S5. Whereas this mechanism of momentum transfer is qualitatively consistent with that suggested by the two-dimensional simulations of bacterial suspensions from Angelani et al. (24), our experiments indicate that it applies to the regime of collective swimming.

Next, we consider the energetic of gear rotation. By analogy to molecular gases, the tangential stress σ acting on the gear due to collisions with bacteria can be approximated as $\sigma \sim knT_{\text{eff}}$ where $T_{\text{eff}} \sim \langle u^2 \rangle$ is average kinetic energy of bacterial motion ("effective temperature"), u is the swimming velocity, n is the concentration of bacteria, and k is a coefficient that depends on the asymmetry of the gear and specificity of bacteria–gear interaction (tumbling rate, shape of the teeth, etc.; note that in equilibrium thermodynamic systems, $k = 0$). On the other hand, the total torque acting on the gear is $Q \sim kha^2 nT_{\text{eff}}$, where a is gear radius and h is its thickness. This torque is balanced by the viscous torque $f_r\Omega$, where Ω is angular velocity. For a gear approximated as a thin disk of radius a in the bulk of the fluid and in the low-Reynolds-number limit, the rotational drag can be written (37) as $f_r \sim 32/3\nu_0 a^3$, with ν_0 being the dynamic viscosity of pure medium. Equating Q with $f_r\Omega$ we then obtain that the rotation rate scales as $\Omega \sim a^{-1}nT_{\text{eff}} = a^{-1}n\langle u^2 \rangle$—that is, inversely with the gear radius and quadratically with the average square velocity of the

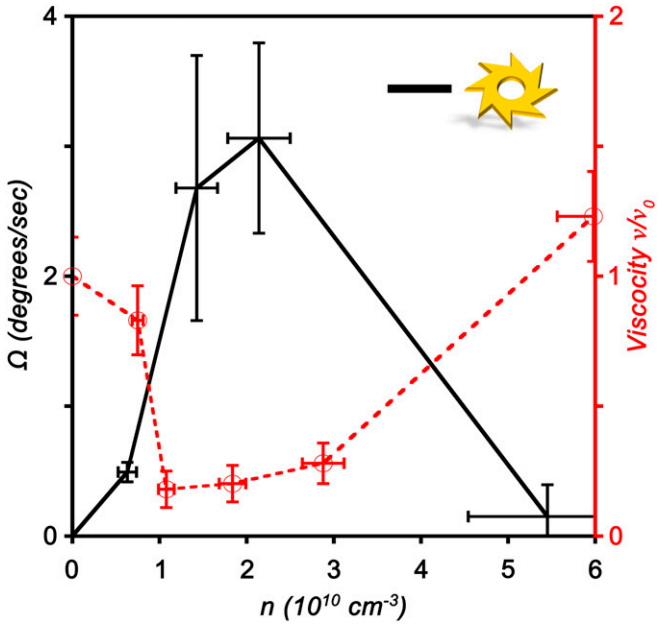

Fig. 4. Concentration dependence. Black solid line has the dependence of the gear rotation rate on the concentration of bacteria, n. Vertical error bars represent standard deviations of the rotation rate with gears decorated with 8 outward teeth. Sharp increase in the rotation rate at concentration $\sim 10^{10}$ cm^{-3} coincides with the onset of collective motion. For concentration above 4×10^{10} cm^{-3} rotation ceases due to the decrease in bacterial motility (32). For comparison, the dependence of effective viscosity ν of bacterial suspension measured at the same conditions is plotted as a red dashed line (adopted from ref. 32); ν_0 is viscosity of liquid without bacteria.

bacteria. Previous studies revealed that at high concentrations the typical velocity of collective flows is roughly five times larger than that of individual bacteria (33, 35). It follows that collective swimming increases the rotation speed at least by a factor of 20. This circumstance probably explains why no rotation is observed in the dilute limit. Finally, we consider how much power, W_g, a gear can extract from the chaotic motion of bacteria. This power can be estimated as $W_g \sim f_r \Omega^2$ that for typical experimental values, $a \sim 200$ μm and $\Omega \sim 1/10$ rad/sec, gives $W_g \sim 10^{-15}$ W, i.e. in the order of femtowatt. Because one bacterium delivers power on the order $W_b \sim f_b u^2 \sim 10^{-17}$ W (f_b is translational viscous drag coefficient for a single bacterium), we conclude that at least hundreds of bacteria are needed to rotate one microgear.

Of course, femtowatt powers are orders of magnitude too small to operate any real-world machines. Still, we believe that the ability of bacteria to actuate submillimeter objects can provide basis for micromanipulation/positioning techniques, or for operating the movable parts of microfluidic circuits (micromixers, separators, etc.). On the fundamental level, our work emphasizes the importance of strong fluctuations that are due to collective bacterial swimming and manifest themselves by the formation of large-scale swirls, "jets," and plumes (31). Collective motion of bacteria also introduces additional time and length scales associated with these large-scale structures. For the conditions of our experiment, the coherent structures (vortices, plumes) are 50–100 μm in size and are characterized by correlation times on the order of 5–7 sec. Thus, the length scale of these structures is still significantly smaller than the size of gears (~400 μm). These large hydrodynamic structures can, however, effectively filter out small-scale fluctuations associated with the motions

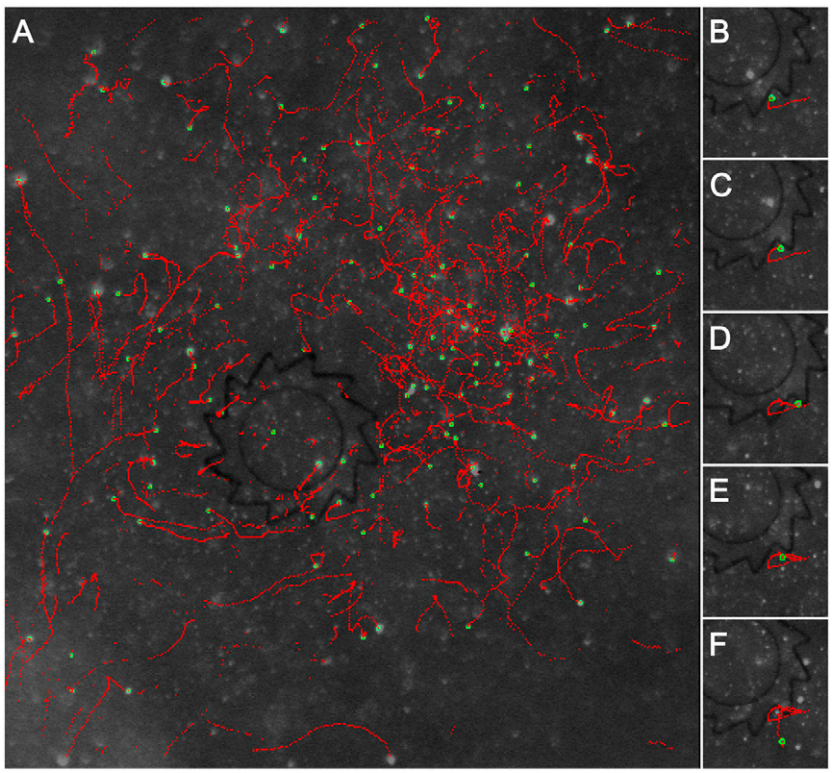

Fig. 5. Tracer trajectories. Trajectories of 2.5 μm fluorescent tracers (green points) tracked in 180 consecutive frames (total tracking time 18 sec). Red curves represent reconstructed tracer trajectories (*A*). Trajectory of an individual tracer in the vicinity of gear's tooth for 5 periods of time, $t = 0$, 5, 10, 15, 20 sec (*B–F*). The tracer spends significant amount of time trapped in the corner before it finally "escapes." For all images, concentration of bacteria is 2×10^{10} cm^{-3}. Movie S5 accompanies this figure.

of individual bacteria (5 μm) and can amplify fluctuations comparable with the sizes of the microparticles/gears to be powered up.

Materials and Methods

Bacteria and Films. Experiments were performed using strain 1085 of *Bacillus subtilis*, which is a rod-shaped bacterium ∼5 μm long and ∼0.7 μm in diameter. The bacteria were grown in a Terrific Broth (TB) medium (Sigma T5574), concentrated by centrifugation, and then placed in a fresh TB medium at average concentration $\sim 2 \times 10^{10}$ cm^{-3}. The computer-controlled experimental setup of a free-standing film of adjustable thickness was based on an earlier design mounted on the moving stage of an inverted microscope (35). Briefly, a 10 μl drop of bacterial suspension was placed between two crossed pairs of fibers that formed a small "window frame" (see Fig. 1*B*). By moving the frame, the drop was stretched out until it formed a ~ 7 mm $\times$ 7 mm film of thickness ∼200 μm. The velocities of aerobic bacteria in the film were controlled by the concentration of oxygen or nitrogen filling the experimental chamber.

Gears and Imaging. Gears were fabricated via standard photolithography. First, SU-8 photoresist (MicroChem Corporation) was spun and baked onto an atomically flat [100] silicon wafer (Monto Silicon Technologies, Inc.). Using a photomask with the desired gear design, the coated wafer was exposed to UV radiation (150 mJ/cm^2). The wafer was then developed in ∼50 mL of propylene glycol monomethyl ether acetate (Sigma-Aldrich) under constant stirring, then washed with both deionized (DI) water and ethanol, and finally dried under stream of nitrogen or air. Gears were removed from the wafer by mechanical shaking overnight in ∼20 mL of acetonitrile. After removal and solvent evaporation, the gears were washed with DI water (four to five times), and then stored in 10 mL of DI water. The gears were placed into the bacteria-containing film using a micropipette. Bright field microscope images were recorded by high-sensitivity CCD camera (Spot Boost EMCCD 2100, Diagnostic Instruments Inc). Orientations and locations of the gears and fluorescent tracer particles trajectories were extracted from the recorded images by in-house tracking software based on MatLab.

ACKNOWLEDGMENTS. The work of I.S.A. and A.S. was supported by the U.S. Department of Energy, Office of Basic Energy Sciences, Division of Materials Science and Engineering, under Contract DEAC02-06CH11357. B.A.G. and M.M.A. gratefully acknowledge financial support from Northwestern University's Nonequilibrium Energy Research Center, one of the U.S. Department of Energy's Energy Frontier Research Centers under Award DESC0000989.

1. Feynman RP (1963) *The Feynman lectures on physics* (Addison-Wesley, Reading).
2. Van den Broeck C, Kawai R, Meurs P (2004) Microscopic analysis of a thermal Brownian motor. *Phys Rev Lett*, 93:090601.
3. Lee SH, Grier DG (2005) One-dimensional optical thermal ratchets. *J Phys-Condens Matter*, 17:S3685–S3695.
4. Lee CS, Janko B, Derenyi I, Barabasi AL (1999) Reducing vortex density in superconductors using the 'ratchet effect'. *Nature*, 400:337–340.
5. Rousselet J, Salome L, Ajdari A, Prost J (1994) Directional motion of Brownian particles induced by a periodic asymmetric potential. *Nature*, 370:446–448.
6. Linke H, et al. (1999) Experimental tunneling ratchets. *Science*, 286:2314–2317.
7. van Oudenaarden A, Boxer SG (1999) Brownian ratchets: Molecular separations in lipid bilayers supported on patterned arrays. *Science*, 285:1046–1048.
8. Villegas JE, et al. (2003) A superconducting reversible rectifier that controls the motion of magnetic flux quanta. *Science*, 302:1188–1191.
9. Hiratsuka Y, Tada T, Oiwa K, Kanayama T, Uyeda TQP (2001) Controlling the direction of kinesin-driven microtubule movements along microlithographic tracks. *Biophys J*, 81:1555–1561.
10. Matthias S, Muller F (2003) Asymmetric pores in a silicon membrane acting as massively parallel Brownian ratchets. *Nature*, 424:53–57.
11. Smoluchowski M (1912) Experimental proof of regular thermodynamic conflicting molecular phenomenons. *Phys Z*, 13:1069–1080.
12. Hanggi P, Marchesoni F (2009) Artificial Brownian motors: Controlling transport on the nanoscale. *Rev Mod Phys*, 81:387–442.
13. Astumian RD (1997) Thermodynamics and kinetics of a Brownian motor. *Science*, 276:917–922.
14. Astumian RD, Hanggi P (2002) Brownian motors. *Phys Today*, 55:33–39.
15. Wambaugh JF, Reichhardt C, Olson CJ, Marchesoni F, Nori F (1999) Superconducting fluxon pumps and lenses. *Phys Rev Lett*, 83:5106–5109.
16. Alberts B, et al. (2002) *Molecular biology of the cell* (Garland Science, New York, NY), 4th ed.
17. Berg HC (1983) *Random walks in biology* (Princeton Univ Press, Princeton, NJ).
18. Galajda P, Keymer J, Chaikin P, Austin R (2007) A wall of funnels concentrates swimming bacteria. *J Bacteriol*, 189:8704–8707.
19. Mahmud G, et al. (2009) Directing cell motions on micropatterned ratchets. *Nature Phys*, 5:606–612.
20. Hiratsuka Y, Miyata M, Tada T, Uyeda TQP (2006) A microrotary motor powered by bacteria. *Proc Natl Acad Sci USA*, 103:13618–13623.
21. Pelling AE, Sehati S, Gralla EB, Valentine JS, Gimzewski JK (2004) Local nanomechanical motion of the cell wall of *Saccharomyces cerevisiae*. *Science*, 305:1147–1150.
22. Liu H, et al. (2002) Control of a biomolecular motor-powered nanodevice with an engineered chemical switch. *Nature Mater*, 1:173–177.
23. Soong RK, et al. (2000) Powering an inorganic nanodevice with a biomolecular motor. *Science*, 290:1555–1558.
24. Angelani L, Di Leonardo R, Ruocco G (2009) Self-starting micromotors in a bacterial bath. *Phys Rev Lett*, 102:048104.
25. Goel A, Vogel V (2008) Harnessing biological motors to engineer systems for nanoscale transport and assembly. *Nature Nanotechnol*, 3:465–475.
26. Kim MJ, Breuer KS (2008) Microfluidic pump powered by self-organizing bacteria. *Small*, 4:111–118.
27. van den Heuvel MGL, Dekker C (2007) Motor proteins at work for nanotechnology. *Science*, 317:333–336.
28. Kaehr B, Shear JB (2009) High throughput design of microfluidics based on directed bacterial motility. *Lab Chip*, 9:2632.
29. Berg HC (2004) *E. Coli in motion* (Springer-Verlag, New York).
30. Wu XL, Libchaber A (2000) Particle diffusion in a quasi-two-dimen sional bacterial bath. *Phys Rev Lett*, 84:3017–3020.
31. Sokolov A, Goldstein RE, Feldchtein FI, Aranson IS (2009) Enhanced mixing and spatial instability in concentrated bacterial suspensions. *Phys Rev E*, 80:031903.
32. Sokolov A, Aranson IS (2009) Reduction of viscosity in suspension of swimming bacteria. *Phys Rev Lett*, 103:148101.
33. Dombrowski C, Cisneros L, Chatkaew S, Goldstein RE, Kessler JO (2004) Self-concentration and large-scale coherence in bacterial dynamics. *Phys Rev Lett*, 93:098103.
34. Zang HP, Be'er A, Smith RS, Florin E-L, Swinney HL (2009) Swarming dynamics in bacterial colonies. *Europhys Lett*, 87:48011.
35. Sokolov A, Aranson IS, Kessler JO, Goldstein RE (2007) Concentration dependence of the collective dynamics of swimming bacteria. *Phys Rev Lett*, 98:158102.
36. Stewart PS, Franklin MJ (2008) Physiological heterogeneity in biofilms. *Nat Rev Microbiol*, 6:199–210.
37. Kim S, Karrila SJ (1991) *Microhydrodynamics: Principles and selected applications* (Dover Publications, New York).